The Role of the Order−Disorder Transition Temperature of Block Copolymer in the Compatibilization of Two Immiscible Homopolymers

Seung Bum Chun and Chang Dae Han*

Department of Polymer Engineering, The University of Akron, Akron, Ohio 44325-0301

Received October 26, 1998; Revised Manuscript Received April 13, 1999

ABSTRACT: The important role that the order−disorder transition temperature (T_{ODT}) of a block copolymer plays in the compatibilization of two immiscible homopolymers is demonstrated, using the model ternary blend systems consisting of a polystyrene-*block*-polybutadiene (SB diblock) copolymer and two immiscible homopolymers, polystyrene (hPS) and polyisoprene (hPI). For the study, SB diblock copolymers having different microstructures were employed. We investigated via transmission electron microscopy (TEM) the morphology of the blends. We found that an SB diblock copolymer was very poorly distributed at the interface between hPS and hPI in an hPS/hPI/SB ternary blend when the specimen was annealed at a temperature below the T_{ODT} of the block copolymer, while a more uniform distribution of the SB diblock copolymer was observed when a specimen was annealed at a temperature above its T_{ODT}. We have shown that the miscibility (or the interaction parameter) between the hPI and PB block in an SB diblock copolymer plays a decisive role in controlling the morphology at the interfaces between hPS and hPI. We conclude that a block copolymer must be designed, such that its T_{ODT} is below the targeted melt blending temperature, in order for the block copolymer to be able to act as an effective compatibilizing agent for two immiscible homopolymers. This conclusion is supported further by investigating the tensile properties and morphology of ternary blends consisting of polypropylene (PP), hPS, and polystyrene-*block*-poly(ethylene-*co*-1-butene)-*block*-polystyrene (SEBS triblock) copolymer (Kraton G1650), which were prepared by melt blending at 200 °C in a batch mixer. That is, little improvement in the tensile properties of the ternary blends was observed when Kraton G1650 was added to PP/hPS binary blends. This observation is explained by a very poor distribution, observed by TEM, of Kraton G1650 at the interface between PP and hPS in the ternary blend. This is attributed to the very high T_{ODT}, estimated to be above 350 °C from currently held mean-field theory, of Kraton G1650 compared to the melt blending temperature employed.

Introduction

A block copolymer, when properly designed in terms of chemical structure, architecture, and molecular weight, can be used as an effective compatibilizing agent for a pair of immiscible homopolymers. During the past decade, a number of research groups reported on compatibilization of two immiscible homopolymers, theoretically[1−7] and experimentally.[8−22] Some researchers[23−25] investigated the adhesion between two immiscible homopolymer layers in the presence of a diblock copolymer in between, and still others[26,27] investigated fracture mechanisms and the interface toughness of two immiscible homopolymers layers in the presence of a diblock copolymer in between.

Notwithstanding much effort spent on the subject during the past decade, our understanding of the subject is still far from complete. To illustrate the point, let us confine our attention to a ternary blend consisting of a pair of homopolymers, A and B, and a block copolymer, C-*block*-D, i.e., A/B/(C-*block*-D) blend. Note that such a ternary blend is general enough to cover special cases: (i) A/B/(A-*block*-B) blend, (ii) A/B/(C-*block*-B) blend, and (iii) A/B/(A-*block*-D) blend. Needless to state, there are many conceivable A/B/(C-*block*-D) blends in terms of the chemical structures and molecular weights of the constituent components (A, B, C, and D), which in turn determine the miscibility between a particular pair of components. To make the situation more complicated, the block length ratio of A-*block*-B, C-*block*-B, or A-*block*-D copolymer, when mixed with a pair of homopolymers, also plays an important role in determining its effectiveness as compatibilizing agent. In this regard, a comprehensive theory is most welcome in order to minimize the number of experiments, which otherwise would have to be performed. To the best of our knowledge, however, at present no comprehensive theory exists in the literature dealing with this subject.

In the experimental studies on compatibilization of two immiscible homopolymers using a block copolymer, for instance, Paul and co-workers[8−12] published a series of papers, reporting an improvement of some mechanical properties of binary blends of polystyrene (hPS) with high-density polyethylene (HDPE) or low-density polyethylene (LDPE) in the presence of a polystyrene-*block*-poly(ethylene-*co*-1-butene)-*block*-polystyrene (SEBS triblock) copolymer, which is a hydrogenated polystyrene-*block*-polybutadiene-*block*-polystyrene (SBS triblock) copolymer. However, they did not investigate the morphology of the ternary blends at the interface between SEBS triblock copolymer and homopolymer. Fayt et al.[14] reported that the addition of polystyrene-*block*-poly(ethylene-*co*-1-butene) (SEB diblock) copolymer to binary blends of LDPE and hPS significantly enhanced both the ultimate tensile strength and the elongation at break. They attributed the enhanced mechanical properties to the role that SEB diblock copolymer played as an emulsifying agent for LDPE/hPS blends. They noted that SEB diblock copolymers acted as efficient emulsifying agents only when the molecular weights of block sequences were comparable to or higher than the molecular weights of the corresponding homopolymers. If a block copolymer played a role of compatibilizing agent for a pair of immiscible homopolymers, an "interphase" should have been formed where block chains

10.1021/ma981665c CCC: $18.00
Published on Web 05/25/1999

and the corresponding homopolymer chains coexist. Below we will elaborate on the thermodynamic requirements that a block copolymer must meet with if it is going to be an effective compatibilizing agent.

When certain mechanical properties of an immiscible polymer blend were improved in the presence of a block copolymer, the size of the discrete phase in the blend was decreased. This was then interpreted as being due to the lowering of interfacial tension by the block copolymer. Apparently, based on such an interpretation, attempts were made to assess the effectiveness of a block copolymer as compatibilizing agent from measurements of the interfacial tension of a pair of immiscible homopolymers. It should be pointed out that an effective compatibilizing agent must form a sufficiently large "interphase", which would then significantly improve mechanical properties of an immiscible polymer blend.

According to Helfand and Tagami,[28,29] the interfacial thickness d of a pair of immiscible homopolymers of infinite molecular weight can be estimated from

$$d = 2b/(6\chi)^{1/2} \tag{1}$$

where χ is the Flory−Huggins interaction parameter and b is the Kuhn statistical length of the two polymers. They also derived the expression for the interfacial tension γ

$$\gamma = (\chi/6)^{1/2} b\rho_0 k_B T \tag{2}$$

in terms of χ, where k_B is the Boltzmann constant, T is the absolute temperature, and ρ_0 is the inverse of monomeric volume of a reference component. Recently, Broseta et al.[30] extended the Helfand−Tagami theory to finite molecular weight of polymers and concluded that, for finite molecular weights, the interfaces are broader and the interfacial tensions smaller than predicted by the assumption of infinite molecular weights of the constituent polymers. They noted that in polydisperse systems small chains accumulate slightly at the interface, lowering the interfacial tension. Within the spirit of mean field approach, from eqs 1 and 2 one can conclude that the smaller the value of χ, the larger the value of d and the smaller the value of γ. Such a conclusion might have led some investigators to further conclude that a block copolymer played the role of an effective compatibilizing agent when it decreased the domain size of the dispersed phase in a two-phase polymer blend. We hasten to point out, however, that eqs 1 and 2 are only valid for a pair of immiscible polymers and not for a ternary blend in which a third component (e.g., a block copolymer) is present in a blend of two immiscible polymers. Moreover, it is clear that eqs 1 and 2 have practical limitations in that d will become exceedingly large, which is physically unacceptable, as the value of χ becomes exceedingly small.

In the literature, it appears that there has been confusion between a dispersing (or emulsifying) agent and a compatibilizing agent. During melt blending of two immiscible polymers, an emulsifying agent can also decrease the interfacial tension, thus decreasing the size of the discrete phase. But, an emulsifying agent does not significantly improve the mechanical properties of an immiscible blend, because the emulsifying agent does not necessarily help the formation of an interphase. Any improvement, which originates from a uniform distribution of finer dispersion, would be marginal. Thus, we can conclude that any attempt to measure the interfacial tension to assess the effectiveness of a compatibilizing agent for a pair of immiscible polymers is not warranted. An effective compatibilizing agent is expected to significantly improve the mechanical properties of an immiscible blend by forming an "interphase" between a homopolymer and a block copolymer. The formation of an interphase must meet with certain thermodynamic requirements. Significant improvement in the mechanical properties of an immiscible blend cannot be achieved without strong interfacial adhesion between the components. To produce a mechanically stable interphase between two immiscible homopolymers in the presence of a block copolymer, the block copolymer must be designed, such that each block has a preferential affinity for each different homopolymer; i.e., the block copolymer must segregate preferentially to the interface between the two immiscible homopolymers.

Although in the past many experimental studies[8−22] were reported on the compatibilization of two immiscible homopolymers, little is mentioned in the literature about the role that the order−disorder transition temperature (T_{ODT}) of a block copolymer plays in the compatibilization. Specifically stated, even when a block copolymer meets with all the thermodynamic requirements for compatibilization of two immiscible homopolymers, the block copolymer would not play the role of an effective compatibilizing agent unless the melt processing temperature is chosen to be above the T_{ODT} of the block copolymer, because an intimate mixing between homopolymers and a microphase-separated block copolymer is not expected to occur at melt processing temperatures below the T_{ODT} of the block copolymer. This means that the molecular weight of a block copolymer must be chosen, such that its T_{ODT} can lie below the melt processing temperature of the blend. A case in point is the use of commercially available SEBS triblock copolymers (e.g., Kraton G series from Shell Development Co.), which have very high molecular weights. For instance, the molecular weight of Kraton G1620 is reported to be 83 700.[21] It should be mentioned that the T_{ODT} of a block copolymer increases with increasing molecular weight. The molecular weights of Kraton G series are so high that no one has been able to measure their T_{ODT}'s before thermal degradation. As will be shown below, the T_{ODT}'s of Kraton G series are estimated to be well above 350 °C, which is much higher than the normal melt processing temperature (say, below 250 °C) of thermoplastic resins (e.g., PS, HDPE, LDPE). Thus, a judicious choice of the molecular weight of a block copolymer is very important if it is going to be used as an effective compatibilizing agent.

The observations made above have motivated us to launch an investigation whether or not the T_{ODT} of a block copolymer would play an important role in the compatibilization of two immiscible homopolymers. For the study, first, we measured the tensile properties of ternary blends consisting of polypropylene (PP), hPS, and a commercial SEBS triblock copolymer, which were prepared by melt blending at 200 °C, far below the T_{ODT} of the SEBS triblock copolymer employed. We observed little improvement in the tensile properties of hPS/PP/SEBS ternary blends when an SEBS triblock copolymer was added to hPS/PP binary blends. This observation is explained by a very poor distribution, observed by transmission electron microscopy (TEM), of the SEBS triblock copolymer at the interface between hPS and PP

Table 1. Molecular Characteristics of Homopolymers Investigated in This Study

sample code	M_n	M_w/M_n	M_w
PS-220[a]	1.10×10^5	2.03	2.23×10^5
PI-200[b]	1.96×10^5	1.07	2.09×10^5
PB-80[c]	7.10×10^4	1.11	7.88×10^4

[a] STYRON 615APR, Dow Chemical Co. [b] It contains 94% 1,4-addition. [c] It contains 91% 1,2-addition. Membrane osmometry was employed to determine number-average molecular weight (M_n), and gel permeation chromatography was used to determine polydispersity M_w/M_n.

in the ternary blend. Next, we prepared via solution blending model ternary blends consisting of hPS, polyisoprene (hPI), and polystyrene-*block*-polybutadiene (SB diblock) copolymer and then annealed the blends for varying periods under isothermal conditions at a temperature above and below the T_{ODT} of the SB diblock copolymer. This was made possible, because the model SB diblock copolymers employed had T_{ODT} below 200 °C. We found distinctly different distributions of SB diblock copolymer, as observed by TEM, between hPS and hPI, depending on the annealing temperatures employed relative to the T_{ODT} of the SB diblock copolymer. In this paper we will report the highlights of our findings. It should be mentioned that the purpose of this paper is to demonstrate, using model ternary blends, our contention that the T_{ODT} of a block copolymer indeed plays a very important role in the compatibilization. Within the limited scope of this paper, we will only present the results of TEM investigation of model ternary blends and interpret the results in terms of T_{ODT} and thermodynamic data, and the discussion of mechanical properties of model ternary blends is beyond the scope of this paper.

Experimental Section

Materials. In this study a commercial grade SEBS triblock copolymer (Kraton G1650, Shell Development Co.) was used, which has the PS block as the minor component (ca. 30 wt %) forming microdomains and poly(ethylene-*co*-1-butene) (PEB) block as the major component forming the matrix. A high molecular weight commercial hPS (STYRON 615APR, Dow Chemical Co.) and a commercial grade of PP (Escorene 1052, Exxon Chemical Co.) were used to blend with Kraton G1650. Ternary blends consisting of hPS, PP, and Kraton G1650 were prepared by melt blending for the purpose of investigating the effectiveness of Kraton G1650 as compatibilizing agent.

To prepare model ternary blends, we synthesized, via anionic polymerization, hPI and polybutadiene (hPB). The molecular characteristics of the homopolymers are summarized in Table 1. We also synthesized, via anionic polymerization, polystyrene-*block*-polyisoprene (SI diblock) and SB diblock copolymers. In the synthesis of SB diblock copolymer we varied the microstructure of PB block having (i) 9% 1,2-addition (SB-14/11), (ii) 44% 1,2-addition (SB-13/12), and (iii) 89% 1,2-addition (SB-9/8), all having lamellar microdomains. The molecular characteristics of the block copolymers are summarized in Table 2. Membrane osmometry (Jupiter Instrument) was used to determine the number-average molecular weight (M_n) of each of the homopolymers and the model block copolymers synthesized, and gel permeation chromatography (GPC) (Waters) was used to determine the polydispersity (M_w/M_n) of each of the polymers synthesized. Using combinations of the homopolymers summarized in Table 1 and the diblock copolymers summarized in Table 2, we prepared, via rapid precipitation, the following ternary systems: (i) hPS/hPI/SB, (ii) hPS/hPI/SI, and (iii) hPS/hPB/SB.

Sample Preparation. Samples of hPS/PP/Kraton G1650 blends were compounded at seven different volume ratios, using a batch mixer (Brabender Plasticorder) at 200 °C for 15 min mixing at a rotor speed of 60 rpm. Samples for tensile property measurement were prepared by compression molding the melt-blended polymer in a hot press at 200 °C. The compression-molded specimens were cut into a dumbbell shape. The length, width, and the thickness of dumbbell specimens were 50, 6, and 1 mm, respectively. Samples for model ternary blends were prepared as follows. Two immiscible homopolymers (hPS with hPI or hPS with hPB) with a block copolymer (SI or SB diblock copolymer) were dissolved in a common solvent, toluene, and then the homogeneous solution (2 wt % polymer) was stirred for at least 24 h. Then, the solution was slowly poured into the rapid precipitation setup, which was comprised of a six-blade turbine centrally placed in a perforated draft tube. The rapid precipitation setup was maintained at −78 °C, and the tall form beaker containing both the draft tube and the rotating shaft was charged with methanol. Immediate precipitation of the polymers was observed upon the polymer solution's contact with the circulating methanol pool. The suspension of the precipitated polymers in a liquid blend of toluene and methanol was filtered at room temperature. After filtration, the precipitated polymers were washed several times to remove toluene by methanol. The washed precipitates were dried at room temperature in a fume hood for 1 day and then in a vacuum oven at 40 °C for 1 week to remove residual solvent. All blend samples were then stored in a freezer. The rapidly precipitated blend was annealed in a vacuum oven at a predetermined temperature for varying periods.

Table 2. Molecular Characteristics of Diblock Copolymers Investigated in This Study

sample code	M_n	M_w/M_n	wt % PS	M_w of PS	M_w of PI or PB
SI-9/9[a]	18 000	1.10	51.0	9400	9000
SB-14/11[b]	24 000	1.06	53.9	13700	11700
SB-13/12[c]	23 000	1.09	53.9	13500	12200
SB-9/8[d]	16 700	1.04	52.8	9200	8200

[a] PI block has 94% 1,4-addition. [b] PB block has 9% 1,2-addition. [c] PB block has 44% 1,2-addition. [d] PB block has 89% 1,2-addition. Membrane osmometry was employed to determined number-average molecular weight (M_n), and gel permeation chromatography was used to determine polydispersity M_w/M_n. The weight percent of PS in each block copolymer was determined using nuclear magnetic resonance spectroscopy.

Samples for rheological measurement and TEM for neat block copolymers were prepared by first dissolving a predetermined amount of a block copolymer (10 wt % in solution) in the presence of 0.1 wt % antioxidant (Irganox 1010, Ciba-Geigy Co.) and then slowly evaporating the solvent. The evaporation of solvent was carried out initially in a fume hood at room temperature for a week and then in a vacuum oven at 40 °C for 3 days. The last trace of solvent was removed by drying the sample in a vacuum oven by gradually raising the oven temperature to 80 °C. The drying of the sample was continued until there was no further change in weight. Finally, the sample was annealed at 110 °C for 10 h.

Transmission Electron Microscopy (TEM). Specimens for TEM were cryoultramicrotomed using a Reichert Ultracut S (Leica) microtome equipped with a diamond knife. Sections (50 nm thick) were obtained at −100 °C. A transmission electron microscope (JEM 1200 EX II, JEOL) operated at 120 kV was utilized to observe the images of the specimens. Blend specimens were stained with ruthenium tetroxide (RuO_4) vapor or osmium tetroxide (OsO_4) vapor.

Tensile Properties Measurement. An Instron test machine (model 4204) was used to measure the tensile properties of blend specimens. Tensile tests were conducted at a deformation rate of 50 mm/min at room temperature.

Rheological Measurement. To determine the T_{ODT} of the block copolymers employed in this study, a Rheometrics mechanical spectrometer (model RMS 800) was used in the oscillatory mode with parallel plate fixtures (25 mm diameter). Two different types of experiment were conducted. (1) Dynamic

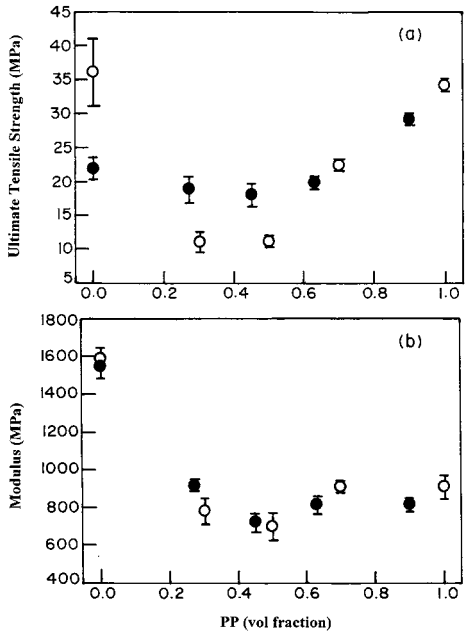

Figure 1. Plots of (a) ultimate tensile strength versus volume fraction of PP and (b) modulus versus volume fraction of PP for (PS-220)/PP/Kraton G1650 ternary blends (●) and (PS-220)/PP binary blends (○).

frequency sweep experiments were conducted for Kraton G1650; i.e., dynamic storage and loss moduli (G' and G'') were measured as functions of angular frequency (ω) ranging from 0.01 to 100 rad/s at temperatures ranging from 190 to 310 °C during heating. The temperature increment in the frequency sweep experiment was 20 °C, and the specimen was kept at a constant temperature for 30−40 min before rheological measurements actually began. (2) Dynamic temperature sweep experiments were conducted for Kraton G1650 and four model diblock copolymers; i.e., G' and G'' were measured under isochronal conditions (at $\omega = 0.01$ rad/s) during heating. The temperature control was accurate to within ±1 °C, and a fixed strain of 0.04 was used at a given temperature, to ensure that measurements were taken well within the linear viscoelastic range of the materials investigated. All the rheological measurements were conducted under a nitrogen atmosphere in order to avoid oxidative degradation of the samples.

Results and Discussion

Tensile Properties of hPS/PP/Kraton G1650 Ternary Blends. Figure 1 gives plots (symbol ●) of ultimate tensile strength (S_b) and modulus (G_m) versus volume fraction of PP (ϕ_{pp}) for (PS-220)/PP/Kraton G1650 ternary blends taken at room temperature. For comparison, plots (symbol ○) of S_b and G_m versus ϕ_{pp} for (PS-220)/PP binary blends are also given in Figure 1. The following observations are worth noting in Figure 1: (i) the ultimate tensile strength of PS-220 (symbol ○ at $\phi_{pp} = 0$) is 36 MPa while the ultimate tensile strength of (PS-220)/Kraton G1650 (10 vol %) binary mixture (symbol ● at $\phi_{pp} = 0$) is 22 MPa, indicating that Kraton G1650 and PS-220 are not miscible; (ii) the addition of Kraton G1650 (10 vol %) increased the ultimate tensile strength of the 65/35 (PS-220)/PP and 50/50 (PS-220)/PP binary blends from ca. 11 to ca. 18 MPa but improved little the ultimate tensile strength of other (PS-220)/PP binary blends; and (iii) the addition of Kraton G1650 (10 vol %) did virtually nothing to improve the modulus of the (PS-220)/ PP binary blends over the entire blend compositions. The above observations indicate that Kraton G1650 did not act as a compatibilizing agent to the (PS-220)/PP binary blends.

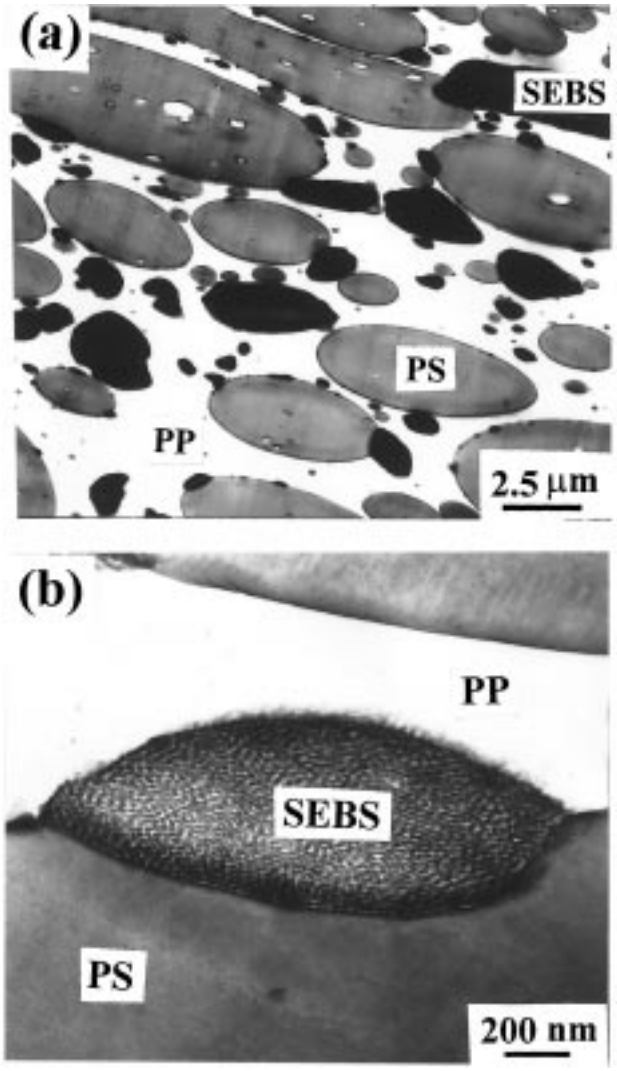

Figure 2. TEM images of 45/45/10 (PS-220)/PP/Kraton G1650 blend: (a) low magnification; (b) high magnification. The white areas represent the PP phase, the light dark areas represent hPS droplets, and the very dark areas represent Kraton G1650.

It is clear from Figure 1 that values of S_b and G_m of (PS-220)/PP/Kraton G1650 ternary blends are lower than the linear additive rule, leading us to speculate that there was little interfacial adhesion between the block copolymer and homopolymers. Below this speculation will be shown to be valid from an independent morphological investigation. We reached the same conclusion from information on elongation at break, which is not presented here.

Morphology of hPS/PP/Kraton G1650 Ternary Blends. To explain the results of the tensile property measurements presented above, we examined the morphology of the ternary blends. The TEM images of the 45/45/10 (PS-220)/PP/Kraton G1650 ternary blend, in which the numbers represent volume percentages, are given in Figure 2, where the white areas represent the PP phase, the light dark areas represent PS-220 droplets, and the very dark areas represent the block copolymer, Kraton G1650. Notice in Figure 2a that Kraton G1650, like PS-220, forms separate domains that are then dispersed in the PP matrix. In Figure 2b, which is a high magnification image of Figure 2a, we observe that a smaller droplet of Kraton G1650 is attached on the surface of the much larger droplet of

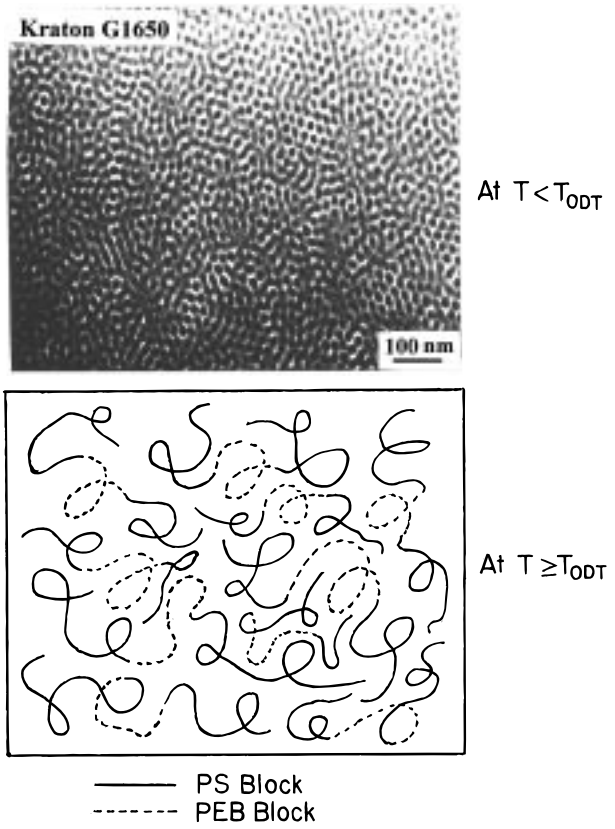

Figure 3. Upper panel: TEM image of Kraton G1650 at $T < T_{ODT}$. Lower panel: schematic describing the disordered state of Kraton G1650 at $T \geq T_{ODT}$.

PS-220, showing no evidence of uniform distribution of Kraton G1650 at the interface between the PS-220 droplet and the PP matrix. The above observation now seems to explain why the tensile properties of the (PS-220)/PP/Kraton G1650 ternary blends are improved little or marginally over those of the (PS-220)/PP binary blends (see Figure 1).

The Origin of the Lack of Significant Improvement of the Tensile Properties of (PS-220)/PP Binary Blends with the Addition of Kraton G1650. The upper panel of Figure 3 gives a TEM image of Kraton G1650, where the white areas represent the PEB block and the dark areas represent the PS block stained by RuO_4. In Figure 3 we observe that the PS block in Kraton G1650 has a hexagonally packed cylindrical microdomain structure. The lower panel of Figure 3 depicts schematically the flexible chains of Kraton G1650 at temperatures equal to or above its T_{ODT}. Note that solubilization between the PS and PEB blocks in Kraton G1650, owing to exhibiting upper critical solution temperature behavior, increases with increasing temperature, giving rise eventually to a homogeneously mixed liquid phase at $T \geq T_{ODT}$.

Figure 4a gives logarithmic plots of G' vs G'' for Kraton G1650 at temperatures ranging from 190 to 310 °C, which were obtained from dynamic frequency sweep experiments. Hereafter, log G' vs log G'' plots will be referred to as Han plots.[31] According to the rheological criterion of Han and co-workers,[35,36] the T_{ODT} of a block copolymer can be determined by the threshold temperature at which Han plots, having a slope of 2 in the terminal region for monodisperse homogeneous polymers, begin to show temperature independence when the dynamic frequency sweep experiment is conducted

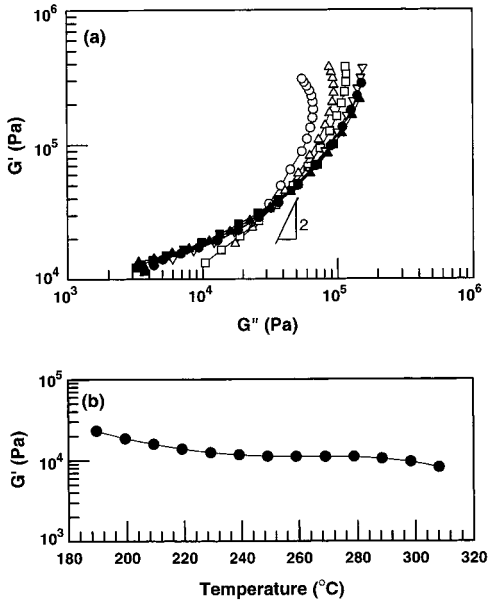

Figure 4. (a) Temperature dependence of Han plots for Kraton G1650 that was obtained from the dynamic frequency sweep experiments during heating at various temperatures: (○) 190, (△) 210, (□) 230, (▽) 250, (●) 270, (▲) 290, and (■) 310 °C. (b) Temperature dependence of dynamic storage modulus G' for Kraton G1650 that was obtained from the dynamic temperature sweep experiments under isochronal conditions during heating.

during heating. Using such a rheological criterion, from Figure 4a we conclude that the T_{ODT} of Kraton G1650 is much higher than 310 °C, the highest experimental temperature employed. Any discussion of the experimental method employed here to determine the T_{ODT} of a block copolymer is beyond the scope of this paper. The interested readers are referred to the original papers.[35]

Figure 4b gives the dependence of storage modulus G' on temperature, which was obtained from the dynamic temperature sweep experiment under isochronal conditions (at $\omega = 0.01$ rad/s), for Kraton G1650. According to the literature,[38,39] the T_{ODT} of a block copolymer can be determined by identifying a temperature at which G' drops precipitously in the plots of G' vs temperature. However, in Figure 4b we observe that the value of G' remains more or less constant over the entire range of temperatures (from 190 to 310 °C) at which the dynamic temperature sweep experiment was performed; i.e., in Figure 4b we cannot identify a critical temperature at which G' drops precipitously. Therefore, we can conclude from Figure 4 that the T_{ODT} of Kraton G1650 is much higher than 310 °C, the highest experimental temperature employed.

Since we could not determine experimentally the T_{ODT} of Kraton G1650, we made an attempt to estimate it using currently held mean-field theory. Using the Helfand−Wasserman theory,[40] we estimated the T_{ODT} of Kraton G1650 to be approximately 350 °C with the following expression

$$\alpha = -0.1678 \times 10^{-2} + 1.2536/T - 0.0648\phi_{PS}/T \quad (3)$$

for the polymer−polymer interaction parameter α for PS/PEB pair reported recently by Han et al.[41] Note that in eq 3 ϕ_{PS} is the volume fraction of PS in a PS/PEB blend, T is the absolute temperature, and the Flory−Huggins interaction parameter χ can be obtained from

Table 3. Comparison of Predicted T_{ODT} (°C) with Measured Value for the Diblock Copolymer Synthesized in This Study

sample code	interaction parameter	predicted T_{ODT}	measd T_{ODT}
SI-9/9	$\alpha = -0.118 \times 10^{-2} + 0.839/T$[a]	147	133
SB-14/11	$\alpha = -0.1576 \times 10^{-2} + 0.917/T + 0.0951\phi_{PS}/T$[b]	176	174
SB-13/12	$\alpha = -0.1814 \times 10^{-2} + 1.048/T + 0.1138\phi_{PS}/T$[c]	192	193
SB-9/8	$\alpha = -0.2388 \times 10^{-2} + 1.355/T + 0.0186\phi_{PS}/T$[d]	142	123

[a] Equation 4 in ref 35c. [b] Equation 13 in ref 41. [c] Equation 10 in ref 41. [d] Equation 14 in ref 41.

the relationship $\chi = \alpha V_r$ with V_r being the molar volume of a reference component. It should be mentioned that eq 3 was obtained for fairly low molecular weights of PS and PEB; namely, $M_w = 1500$ for PS and $M_w = 3880$ for PEB. In view of the fact that α depends on the molecular weight of the constituent components, the estimated $T_{ODT} = 350$ °C for Kraton G1650 may be a very conservative value, because $M_w = 27\,000$ for PS block and $M_w = 63\,000$ for PEB block in Kraton G1650. It is clear then that the T_{ODT} of Kraton G1650 is indeed very high, compared to the melt blending temperature (200 °C) employed in the present study.

We can now understand why, as shown in Figure 2, Kraton G1650 in the 45/45/10 (PS-220)/PP/Kraton G1650 blend, which was melt blended at 200 °C, was not distributed uniformly at the interface between the PS droplet and the PP matrix. This is simply because the melt blending temperature employed was very far below the T_{ODT} of Kraton G1650. This observation is very significant in that in order for a block copolymer to be able to function as an effective compatibilizing agent for a pair of immiscible homopolymers, the block copolymer in terms of molecular weight and block length ratio must be designed in such a way that its T_{ODT} may lie below the intended melt blending (or processing) temperature.

Morphology of Model A/B/(A-*block*-D) Ternary Systems. The (PS-220)/PP/Kraton G1650 ternary blends investigated can be categorized, for our purposes here, as A/B/(A-*block*-D) ternary system although Kraton G1650 is a PS-*block*-PEB-*block*-PS copolymer. To elaborate on the important role that the T_{ODT} of a block copolymer plays in the compatibilization of a pair of immiscible homopolymers, we have investigated the morphologies of model A/B/(A-*block*-D) ternary systems by synthesizing low-molecular-weight A-*block*-D copolymers that would give rise to a relatively low T_{ODT} (lower than 200 °C; see Table 3), namely, an SI diblock copolymer (SI-9/9) and three SB diblock copolymers with varying amounts of 1,2-addition in the PB block: (i) SB-14/11 having 9% 1,2-addition in the PB block, (ii) SB-13/12 having 44% 1,2-addition in the PB block, and (iii) SB-9/8 having 89% 1,2-addition in the PB block. Also, we synthesized an hPI (PI-200) and an hPB (PB-80), the microstructures and molecular weights of which are summarized in Table 1. The rationale behind the synthesis of these SB diblock copolymers having different amounts of 1,2-addition in the PB block will become clear when the morphologies of the model A/B/(A-*block*-D) ternary blends are presented below.

Since our contention here is to demonstrate the extreme importance of the T_{ODT} of a block copolymer in the compatibilization of two immiscible homopolymers,

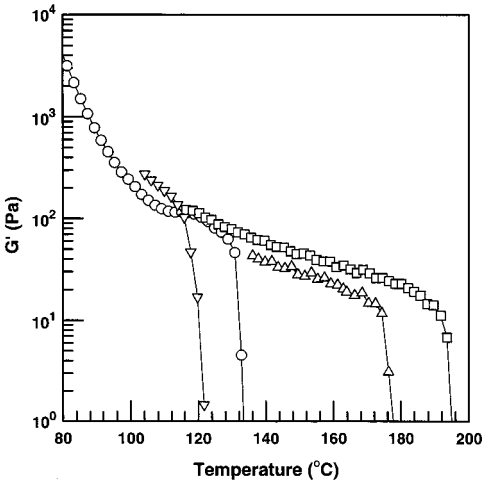

Figure 5. Temperature dependence of dynamic storage modulus that was obtained from the dynamic temperature sweep experiments under isochronal conditions during heating for (○) SI-9/9, (△) SB-14/11, (□) SB-13/12, and (▽) SB-9/8.

we conducted dynamic temperature sweep experiments under isochronal conditions (at $\omega = 0.01$ rad/s) in order to determine the T_{ODT} of each of the four model diblock copolymers synthesized in this study: SI-9/9, SB-14/11, SB-13/12, and SB-9/8. The results of such experiments are given in Figure 5, in which we can identify a critical temperature at which the value of G' drops precipitously for each diblock copolymer, and thus we can determine the T_{ODT} of each diblock copolymer, as summarized in Table 3. For comparison, we estimated the T_{ODT} of each of the four model diblock copolymers using the Helfand–Wasserman theory,[40] and they are also given in Table 3. It is gratifying to observe in Table 3 that the agreement between experiment and prediction is very reasonable, in the light of some questionable assumptions made in the Helfand–Wasserman theory and some uncertainties associated with the polymer–polymer interaction parameters employed in the prediction.

Figure 6 gives the TEM images of as-precipitated ternary blends: (a) 63/27/10 (PS-220)/(PI-200)/(SB-14/11), (b) 63/27/10 (PS-220)/(PI-200)/(SB-13/12), and (c) 63/27/10 (PS-220)/(PI-200)/(SB-9/8), in which the numbers represent weight percentages. It should be mentioned that the as-precipitated blends were in the form of powders. Specimens for taking TEM images were prepared by first embedding as-precipitated powders in an epoxy (EPON 828) and curing it for about 24 h at room temperature using 10 wt % triethylenetetramine. The embedded samples were then ultramicrotomed using a microtome equipped with a diamond knife. The micrographs in Figure 6 will be very useful to interpret the morphology of the model ternary blends after annealing under isothermal conditions; i.e., the micrographs in Figure 6 will serve as a reference for later discussion. Note in Figure 6 that the white areas represent PS-220 and the light dark areas represent PI-200. Due to the low magnification, it is not possible to identify in Figure 6 SB diblock copolymer in the ternary blends. It is worth noting in Figure 6 that the as-precipitated blends have a co-continuous morphology, very similar to that observed in previous studies of Yang and Han,[42] who prepared binary blends of hPS and hPI by rapid precipitation, and Lee and Han,[43] who prepared binary blends of hPS and poly(methyl methacrylate) by rapid

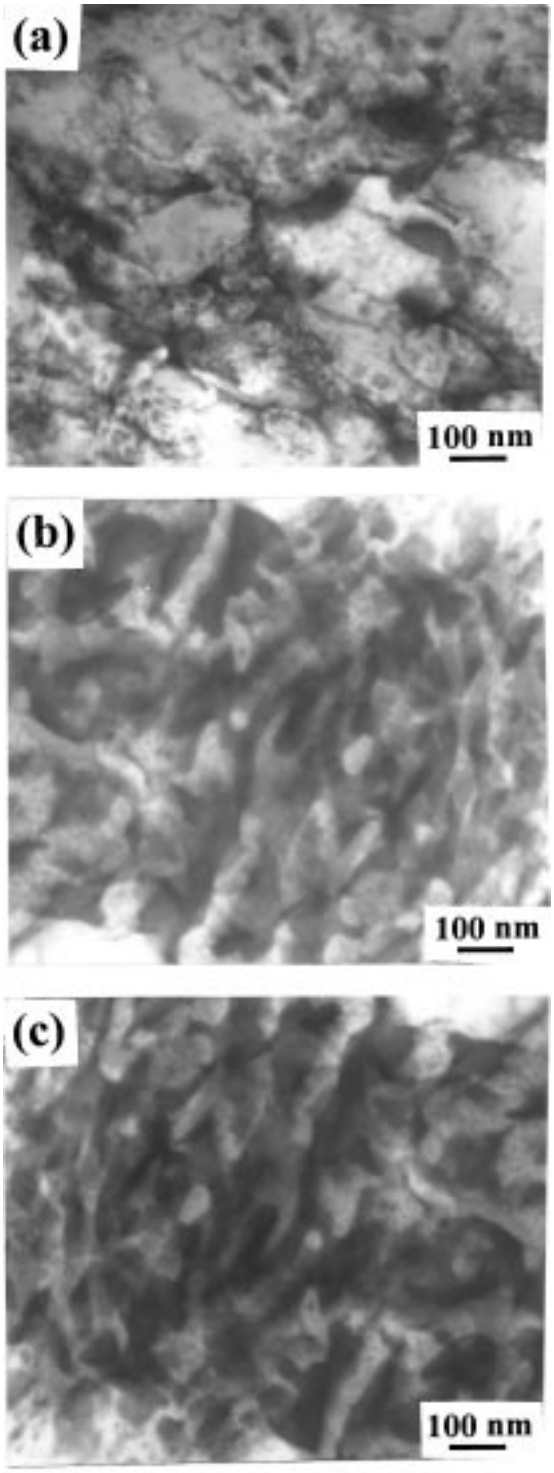

Figure 6. TEM images of as-precipitated ternary blends: (a) 63/27/10 (PS-220)/(PI-200)/(SB-14/11); (b) 63/27/10 (PS-220)/(PI-200)/(SB-13/12); (c) 63/27/10 (PS-220)/(PI-200)/(SB-9/8).

precipitation. As elaborated on previously,[42,43] rapid precipitation may be regarded as being "composition quenching", and phase separation by rapid precipitation via composition quenching is equivalent to that by spinodal decomposition via temperature quenching.

The TEM images of the 63/27/10 (PS-220)/(PI-200)/(SB-14/11) blend annealed at 190 °C (above the T_{ODT} of SB-14/11) for 12 h are given in the upper panel of Figure 7 (a and b). At a low magnification (Figure 7a) we observe a dispersed two-phase morphology in which droplets of PI-200 (the light dark areas) and SB-14/11 (the darker areas) are dispersed in the PS-220 (the white areas). At a high magnification (Figure 7b) we observe a large PI-200 droplet that is uniformly covered by the block copolymer SB-14/11 and also smaller droplets of macrophase-separated SB-14/11 droplets. The TEM images of the 63/27/10 (PS-220)/(PI-200)/(SB-14/11) blend annealed at 160 °C (below the T_{ODT} of SB-14/11) for 12 h are given in the lower panel of Figure 7 (c and d). At a low magnification (Figure 7c) we observe a dispersed two-phase morphology in which droplets of PI-200 (the light dark areas) and SB-14/11 (the darker areas) are dispersed in the PS-220 matrix (the white areas). At a high magnification (Figure 7d) we observe part of the added block copolymer SB-14/11 (having lamellar microdomains) staying unevenly at the surface of a PI-200 droplet. Notice the difference in the thickness of SB-14/11 layer, at the same magnification, on the surface of a PI-200 droplet in two situations: one annealed at $T > T_{ODT}$ of SB-14/11 (Figure 7b) and the other annealed at $T < T_{ODT}$ of SB-14/11 (Figure 7d). This observation clearly demonstrates the importance of the T_{ODT} of a block copolymer in the compatibilization of a pair of immiscible homopolymers.

It is worth noting from a comparison of Figure 7 with Figure 6a that, during isothermal annealing, the co-continuous morphology of the as-precipitated 63/27/10 (PS-220)/(PI-200)/(SB-14/11) blend transformed into a dispersed morphology. In Figure 7 we observe that after annealing the minor component hPI forms droplets, which are then dispersed in the major component hPS. This observation is consistent with the previous studies of Yang and Han[42] and Lee and Han.[43]

It should be mentioned that the value of χ for a pair of PI having 96% 1,4-addition and PB having 9% 1,2-addition is estimated to be 0.0015 at 190 °C and 0.0013 at 160 °C.[44] Owing to the very small values of χ, though positive, the PI/PB pair may be regarded as being very close to an athermal system. This now may explain the reason why the block copolymer SB-14/11 covered the entire surface of the PI-200 droplet (see Figure 7b) when the annealing temperature was higher than the T_{ODT} of SB-14/11. On the other hand, when the annealing temperature was lower than the T_{ODT} of SB-14/11, neither PS-220 nor PI-200 chains would mix with the lamellar microdomains of PB block in SB-14/11.

The TEM images of the 63/27/10 (PS-220)/(PI-200)/(SB-13/12) blend annealed at 207 °C (above the T_{ODT} of SB-13/12) for 12 h are given in the upper panels of Figure 8 (a and b). It should be remembered that the PB block in SB-13/12 has 44% 1,2-addition, while the PB block in SB-14/11 has 9% 1,2-addition (see Table 2). At a low magnification (see Figure 8a) we observe (i) a dispersed two-phase morphology in which droplets of PI-200 (the light dark areas) and SB-13/12 (the darker areas) are dispersed in the PS-220 matrix (the white areas) and (ii) part of the added block copolymer SB-13/12 entered into a PI-200 droplet and was distributed unevenly inside the droplet. At a high magnification (see Figure 8b) we observe a large PI-200 droplet having the block copolymer SB-13/12 with microdomain morphology gradually changing from lamellae near the surface of the droplet to spheres deep inside the droplet. This observation indicates that, during the annealing at $T > T_{ODT}$ of SB-13/12 for 12 h, solubilization occurred between the homopolymer PI-200 and the block copoly-

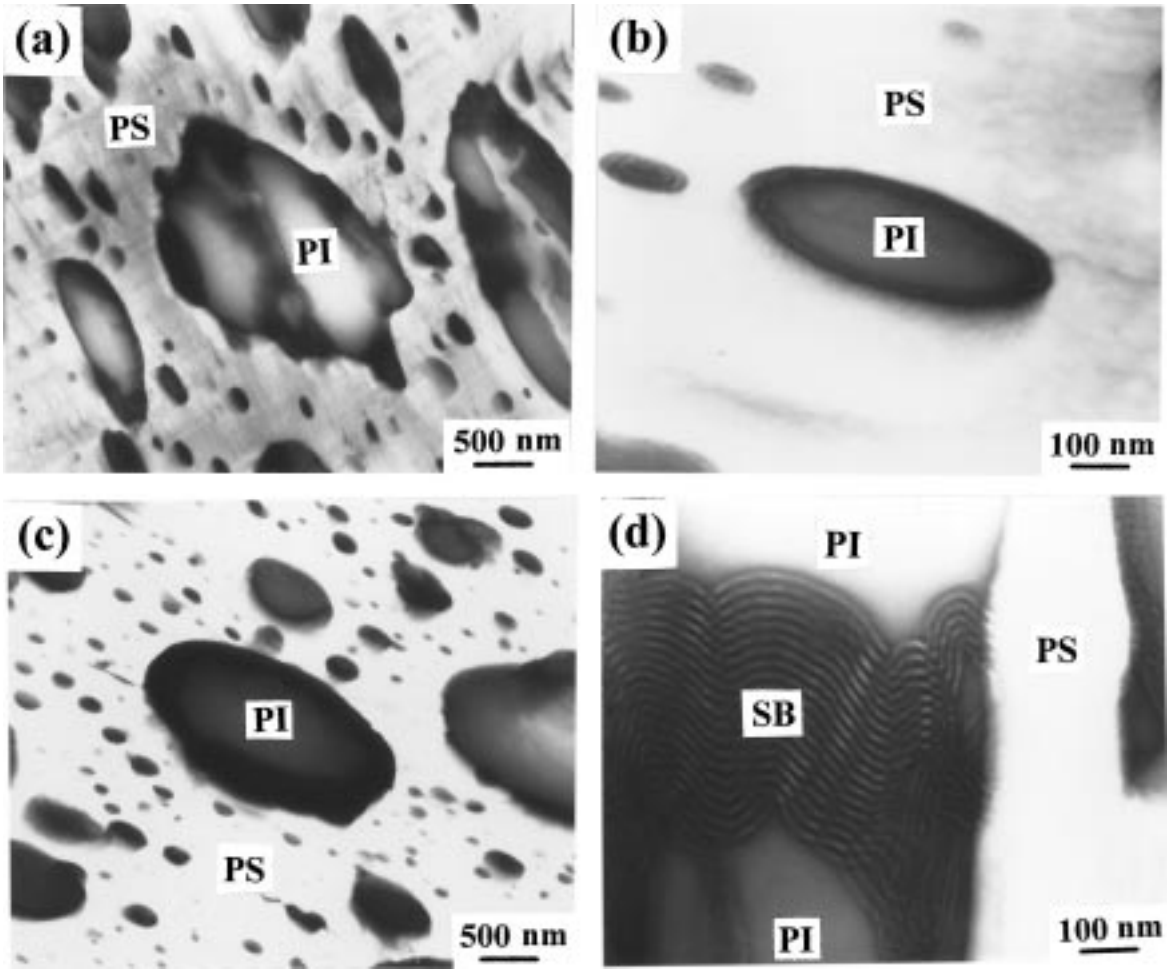

Figure 7. The upper panel describes TEM images of the 63/27/10 (PS-220)/(PI-200)/(SB-14/11) blend annealed at 190 °C (above the T_{ODT} of SB-14/11) for 12 h: (a) at a low magnification, showing a dispersed two-phase morphology in which droplets of PI-200 (the light dark areas) and SB-14/11 (the darker areas) are dispersed in the PS-220 matrix (the white areas); (b) at a high magnification, showing a PI-200 droplet covered completely by SB-14/11 and smaller droplets of macrophase-separated SB-14/11 dispersed in the PS-220 matrix. The lower panel describes TEM images of the 63/27/10 (PS-220)/(PI-200)/(SB-14/11) blend annealed at 160 °C (below the T_{ODT} of SB-14/11) for 12 h: (c) at a low magnification, showing a dispersed two-phase morphology in which droplets of PI-200 (the light dark areas) and SB-14/11 (the darker areas) are dispersed in the PS-220 matrix (the white areas); (d) at a high magnification, showing the presence of SB-14/11 (lamellar microdomains) between a PI-200 droplet and the PS-220 matrix (the white areas).

mer SB-13/12, which was not the case in the 63/27/10 (PS-220)/(PI-200)/(SB-14/11) blend (compare Figure 8b with Figure 7b). The observed difference in morphology between the two ternary blends, 63/27/10 (PS-220)/(PI-200)/(SB-14/11) and 63/27/10 (PS-220)/(PI-200)/(SB-13/12), is attributable to the difference in miscibility between the (PI-200)/(SB-14/11) pair and the (PI-200)/(SB-13/12) pair. Specifically, the (1,4-PI)/(1,4-PB) pair is not miscible (giving rise to positive values of χ),[44,45] while the (1,4-PI)/(1,2-PB) pair is miscible (giving rise to negative values of χ).[44] Therefore, as the amount of 1,2-addition in the PB block of an SB diblock is increased, better miscibility is expected between 1,4-PI and SB diblock copolymer. This observation may now explain the observed difference in morphology between 63/27/10(PS-220)/(PI-200)/(SB-14/11) and 63/27/10 (PS-220)/(PI-200)/(SB-13/12) blends, because the PB block in SB-13/12 has a greater amount of 1,2-addition than the PB block in SB-14/11.

The TEM images of the 63/27/10 (PS-220)/(PI-200)/(SB-13/12) blend annealed at 177 °C (below the T_{ODT} of SB-13/12) for 12 h are given in the lower panels of Figure 8 (c and d). At a low magnification (Figure 8c) we observe a dispersed two-phase morphology in which droplets of PI-200 (the dark areas) are dispersed in the PS-220 matrix (the white areas). At a high magnification (Figure 8d) we observe smaller droplets of block copolymer SB-13/12, maintaining lamellar microdomain structure, inside a larger PI-200 droplet. Observe the totally different morphologies inside a PI-200 droplet between parts b and d of Figure 8. This observation can easily be understood from the point of view of the annealing temperature employed (207 °C vs 177 °C) relative to the T_{ODT} (193 °C) of the block copolymer SB-13/12. That is, when the 63/27/10 (PS-220)/(PI-200)/(SB-13/12) blend was annealed at 177 °C, i.e., below the T_{ODT} of SB-13/12, the miscibility between the PI-200 and microphase-separated PB block in SB-13/12 would be extremely poor, thus giving rise to the morphology displayed in Figure 8d. On the other hand, when the same blend was annealed at 207 °C, i.e., above the T_{ODT} of SB-13/12, the miscibility between the PI-200 and the flexible PB block chains in SB-13/12 would be immensely enhanced, giving rise to the morphology displayed in Figure 8b. Again, the above observation demonstrates how important is the choice of annealing (or processing) temperature, relative to the T_{ODT} of a

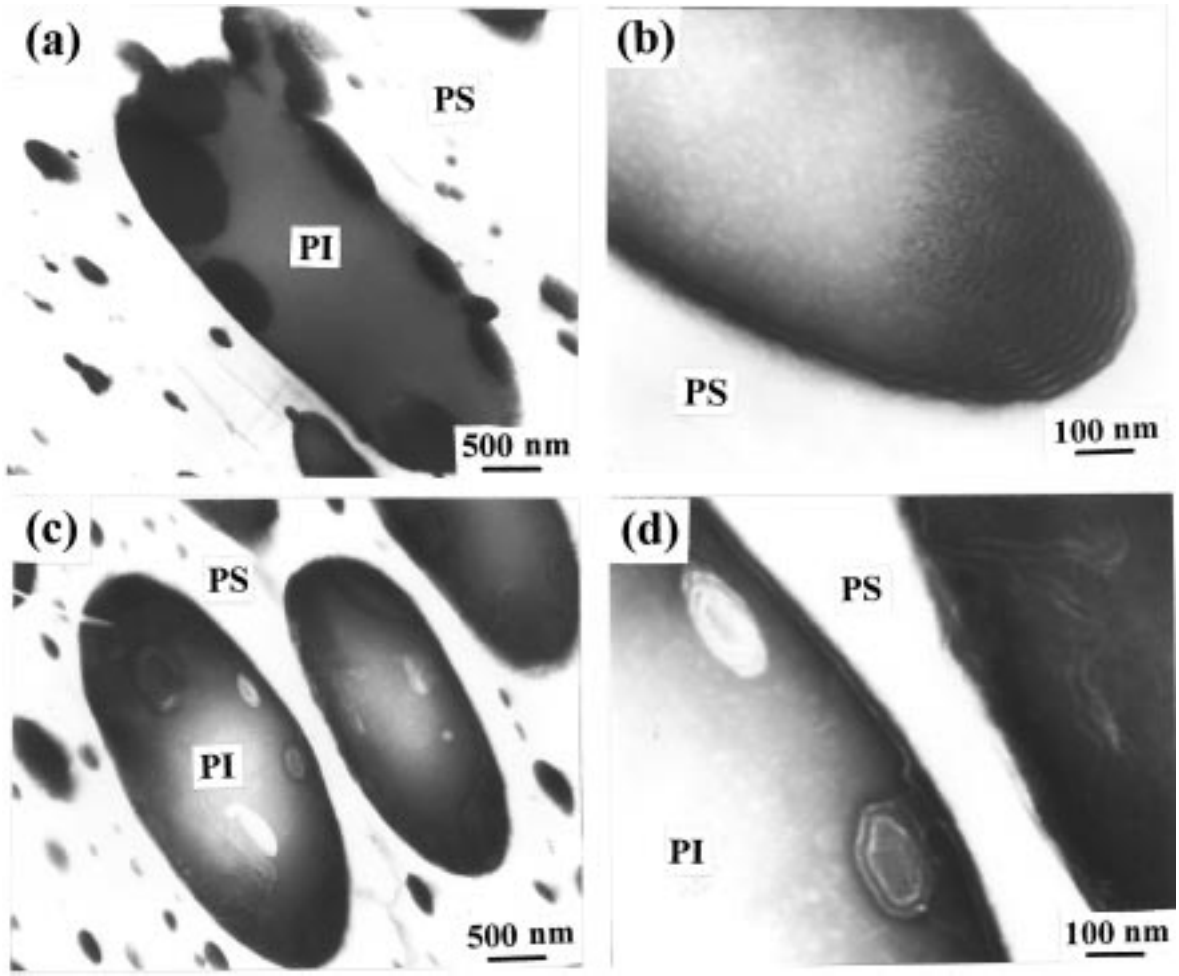

Figure 8. The upper panel describes TEM images of the 63/27/10 (PS-220)/(PI-200)/(SB-13/12) blend annealed at 207 °C (above the T_{ODT} of SB-13/12) for 12 h: (a) at a low magnification, showing a dispersed two-phase morphology in which droplets of PI-200 (the light dark areas) are dispersed in the PS-220 matrix (the white areas) and SB-13/12 (the darker areas) that entered into and distributed nonuniformly inside a PI-200 droplet; (b) at a high magnification, showing a PI-200 droplet having different microdomain morphologies distributed throughout. The lower panel describes TEM images of the 63/27/10 (PS-220)/(PI-200)/(SB-13/12) blend annealed at 177 °C (below the T_{ODT} of SB-13/12) for 12 h: (c) at a low magnification, showing a dispersed two-phase morphology in which droplets of PI-200 (the dark areas) are dispersed in the PS-220 matrix (the white areas); (d) at a high magnification, showing smaller SB-13/12 droplets having lamellar microdomains inside a larger PI-200 droplet.

block copolymer, in the compatibilization of a pair of immiscible homopolymers.

A comparison of Figure 8 with Figure 6b shows that, during isothermal annealing, the co-continuous morphology of the as-precipitated 63/27/10 (PS-220)/(PI-200)/(SB-13/12) blend transformed into a dispersed morphology, and the minor component hPI forms droplets dispersed in the major component hPS, consistent with the previous findings of Han and co-workers.[42,43]

It should be mentioned that the value of χ for a pair of PI having 96% 1,4-addition and PB having 44% 1,2-addition is estimated to be 0.0009 at 207 °C and 0.0005 at 177 °C.[44] Note that the magnitude of these χ values is smaller than that for a pair of PI having 96% 1,4-addition and PB having 9% 1,2-addition given above, indicating that the miscibility between 1,4-PI and PB is enhanced as the amount of 1,2-addition in PB increases. Owing to the very small values of χ, though positive, the PI/PB pair having 96% 1,4-addition in PI and 44% 1,2-addition in PB may be regarded as being very close to an athermal system. This now may explain the reason why the block copolymer SB-13/12 entered into the PI-200 droplet and then solubilized at least in part in the hPI phase, giving rise to spherical microdomains deep inside the hPI droplet and lamellar microdomains near the surface of the hPI droplet. In other words, it is clear that the miscibility between PI-200 and SB-13/12 is greatly enhanced compared to that between PI-200 and SB-14/11 (compare Figure 8b with Figure 7b) when the annealing temperature was higher than the T_{ODT} of the respective block copolymer. This is attributable to the smaller χ value for the (PI-200)/PB block in the SB-13/12 pair compared to that for the (PI-200)/PB block in the SB-14/11 pair. However, when the annealing temperature was lower than the T_{ODT} of SB-13/12, little mixing between SB-13/12 and PI-200 or little solubilization of SB-13/12 in PI-200 occurred (see Figure 8d). This observation points out once again that the T_{ODT} of a block copolymer plays a predominant role in the compatibilization of two immiscible homopolymers.

The TEM images of the 63/27/10 (PS-220)/(PI-200)/(SB-9/8) blend annealed at 160 °C (above the T_{ODT} of SB-9/8) for 12 h are given in the upper panel of Figure 9 (a and b). Note that the PB block in SB-9/8 has 89% 1,2-addition (see Table 2). At a low magnification (see Figure 9a) we observe (i) a dispersed two-phase morphology in which droplets of PI-200 (the light dark

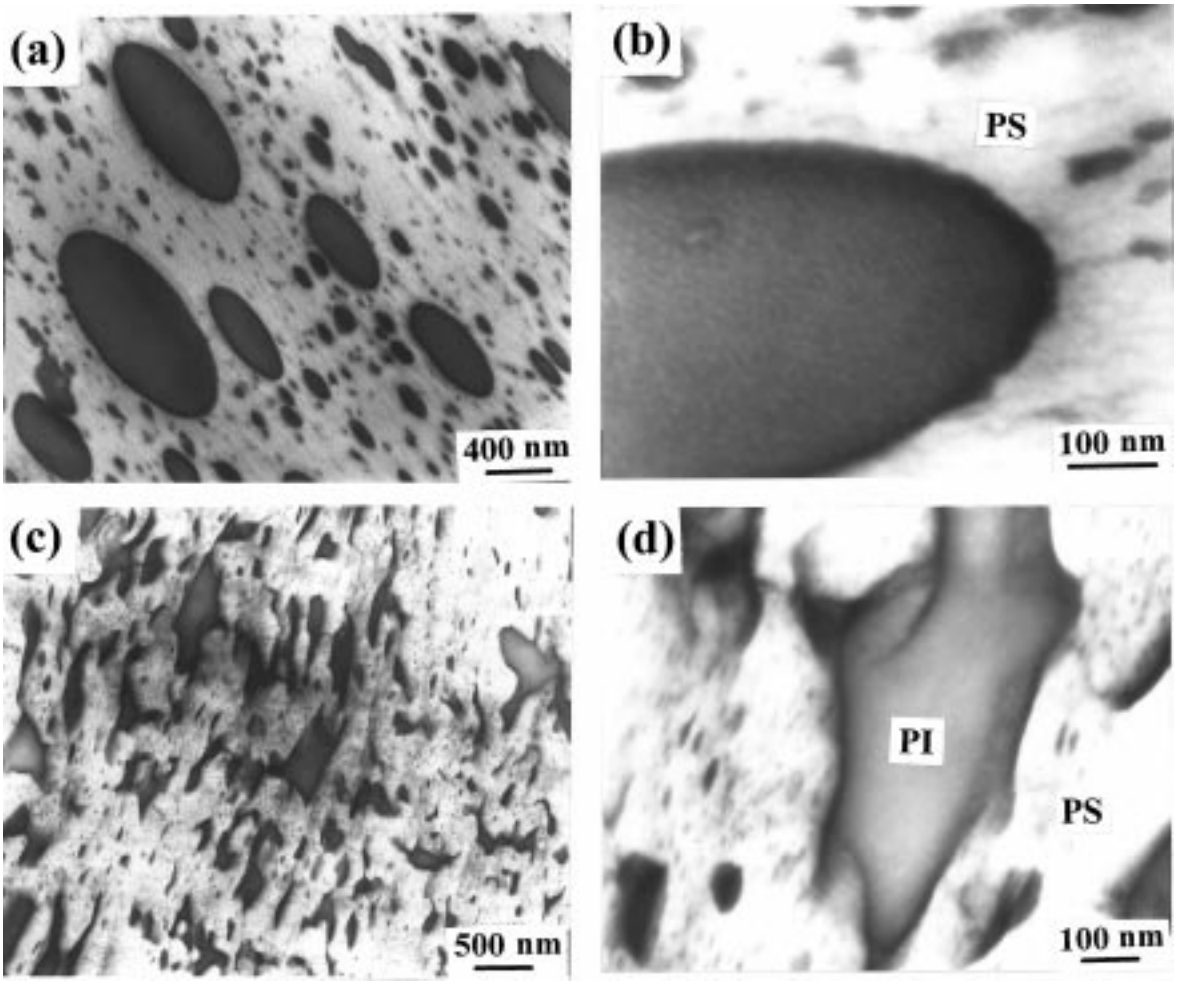

Figure 9. The upper panel describes TEM images of the 63/27/10 (PS-220)/(PI-200)/(SB-9/8) blend annealed at 160 °C (above the T_{ODT} of SB-9/8) for 12 h: (a) at a low magnification, showing a dispersed two-phase morphology in which droplets of PI-200 (the dark areas) are dispersed in the PS-220 matrix (the white areas); (b) at a high magnification, showing a PI-200 droplet having a uniform distribution of spherical microdomains throughout. The lower panel describes TEM images of the 63/27/10 (PS-220)/(PI-200)/(SB-9/8) blend annealed at 110 °C (below the T_{ODT} of SB-9/8) for 12 h: (a) at a low magnification, showing a poorly dispersed two-phase morphology in which droplets of PI-200 (the dark areas) are dispersed in the PS-220 matrix (the white areas); (b) at a high magnification, showing irregularly shaped PI-200 droplets dispersed in the PS-220 matrix and unevenly distributed SB-9/8 on the surface of a PI-200 droplet.

areas) are dispersed in the PS-220 matrix (the white areas) and (ii) PI-200 droplet is surrounded more or less uniformly by the block copolymer SB-9/8 (the darker areas), which is quite different from that made above with reference to Figure 8a. At a high magnification (see Figure 9b) we observe (i) a PI-200 droplet having a uniform distribution of spherical microdomains throughout and (ii) smaller droplets of macrophase-separated SB-9/8 dispersed in the hPS matrix. Notice the difference in morphology between the 63/27/10 (PS-220)/(PI-200)/(SB-13/12) ternary blend (see Figure 8b) and the 63/27/10 (PS-220)/(PI-200)/(SB-9/8) ternary blend (Figure 9b). The observed difference in morphology between the two ternary blends is attributable to the difference of the microstructures of PB block in the respective block copolymers: 44% 1,2-addition in SB-13/12 and 89% 1,2-addition in SB-9/8. That is, during annealing at a temperature above the T_{ODT} of the respective block copolymer, a much faster mixing (or solubilization) between the flexible PB block chains in SB-9/8 and the flexible chains of PI-200 occurred, giving rise to spherical microdomain structure, than between the flexible PB block chains in SB-13/12 and the flexible chains of PI-200.

It should be mentioned that the value of χ for a pair of PI having 96% 1,4-addition and PB having 89% 1,2-addition is estimated to be -0.0017 at 160 °C and -0.0028 at 110 °C,[44] and thus the hPI/hPB pair has attractive interactions. This observation now seems to explain the reason why the block copolymer SB-9/8 is solubilized in the hPI droplet, giving rise to a morphological transformation from lamellae to spheres (see Figure 9b) when the annealing temperature was higher than the T_{ODT} of SB-9/8. In other words, whereas PI-200 chains would not mix with the PB block of SB-9/8 at $T < T_{ODT}$ of SB-9/8, PI-200 chains would mix with the PB block of SB-9/8 at $T > T_{ODT}$ of SB-9/8, swelling the PB block chains to increase the average distance of the neighboring junctions of the block copolymers at the interface. The increase of the junction distance would have decreased the PS microdomain thickness in order to keep the density of PS lamellae constant. Owing to the attractive interactions (i.e., miscibility) between PI-200 and PB block of SB-9/8 at $T > T_{ODT}$ of SB-9/8, a morphological transition occurred from lamellar to spherical microdomain structure. The spherical PS microdomains inside the PI-200 droplets have lost long-

Table 4. Summary of the Flory−Huggins Interaction Parameter χ for PI/PB Pairs Having Different Amounts of 1,2-Addition in PB

polymer pair	χ	annealing temp (°C)
PI[a]/PB-1[b]	0.0013	160
	0.0015	190
PI[a]/PB-2[c]	0.0005	177
	0.0009	207
PI[a]/PB-3[d]	−0.0028	110
	−0.0017	160

[a] PI contains 94% 1,4-addition. [b] PB block of SB-14/11 contains 9% 1,2-addition. [c] PB block of SB-13/12 contains 44% 1,2-addition. [d] PB block of SB-9/8 contains 89% 1,2-addition.

range spatial order, so that they are randomly distributed in the PI-200 phase.

The TEM images of the 63/27/10 (PS-220)/(PI-200)/(SB-9/8) blend annealed at 110 °C (below the T_{ODT} of SB-9/8) for 12 h are given in the lower panels of Figure 9 (c and d). At a low magnification (Figure 9c) we observe a rather poorly dispersed two-phase morphology in which irregularly shaped droplets of PI-200 (the dark areas) are dispersed in the PS-220 matrix (the white areas). The poor state of dispersion in Figure 9c is attributable to the low annealing temperature (110 °C) employed relative to the T_{ODT} (120 °C) of SB-9/8. At a high magnification (Figure 9d) we observe irregularly shaped PI-200 droplets dispersed in the PS-220 matrix, and the block copolymer SB-9/8 appears to be distributed unevenly on the surface of the PI-200 droplet. The observation made in Figure 9 is consistent with that made above with reference to Figures 7 and 8, insofar as the role that the T_{ODT} of a block copolymer plays in the compatibilization of a pair of immiscible homopolymers.

Again, a comparison of Figure 9 with Figure 6c shows that during isothermal annealing the co-continuous morphology of the as-precipitated 63/27/10 (PS-220)/(PI-200)/(SB-9/8) blend transformed into a dispersed morphology, and the minor component hPI forms droplets dispersed in the major component hPS, consistent with the previous findings of Han and co-workers.[42,43]

Concluding Remarks

In this paper we have demonstrated the important role that the T_{ODT} of a block copolymer plays in the effective compatibilization of two immiscible homopolymers. In doing so, we synthesized hPS, hPI, and SB diblock copolymers to prepare model hPS/hPI/SB ternary blends. In the synthesis of SB diblock copolymers we varied the microstructure of the PB block, and we have demonstrated that the miscibility (or the interaction parameter) between the hPI and PB block played a decisive role in controlling the morphology at the interfaces between two immiscible homopolymers, hPS and hPI. Table 4 gives a summary of χ values for the three PI/PB pairs investigated in this study. Specifically, we have shown that the 63/27/10 hPS/hPI/(SB-9/8) blend, which has a very small negative χ value for PI/PB pair, has a uniform distribution of the block copolymer SB-9/8 on the entire surface of hPI droplets (see Figure 9a), while the 63/27/10 PS/hPI/(SB-14/11) and 63/27/10 hPS/hPI/(SB-13/12) blends, each having a very small positive χ value for PI/PB pair, has a very uneven distribution of the block copolymer, SB-14/11 or SB-13/12, on the surface of hPI droplets (see Figures 7a and 8a).

At this juncture it is worth pointing out, with reference to Figures 7−9, that although the value of χ for the PI/PB pair, exhibiting lower critical solution temperature, increases (i.e., the solubility between PI and PB decreases) with increasing temperature, we observe a much improved distribution of a block copolymer (SB-14/11, SB-13/12, or SB-9/8) between hPS and hPI. This can be explained by the fact that the difference in χ value between the two annealing temperatures employed (i.e., at $T < T_{ODT}$ and $T > T_{ODT}$ of the SB diblock copolymer) is rather small, whereas the mobility (i.e., melt viscosity) of the SB diblock copolymer chains at $T > T_{ODT}$ is much greater (at least an order of magnitude) than that at $T < T_{ODT}$. Thus, the improved distribution of the SB diblock copolymer between hPS and hPI is controlled predominantly by the viscosity of the SB diblock copolymer over the difference in χ value between the two annealing temperatures employed.

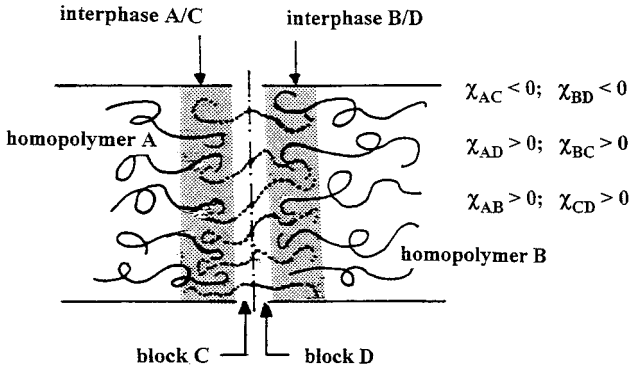

Figure 10. Schematic diagram describing the component distributions in the interfacial region of a ternary blend consisting of homopolymer A, homopolymer B, and C-*block*-D copolymer, in which we have assumed the following relationships hold for the six interaction parameters: $\chi_{AC} < 0$, $\chi_{BD} < 0$, $\chi_{AB} > 0$, $\chi_{AD} > 0$, $\chi_{BD} > 0$, and $\chi_{CD} > 0$.

Contrary to the claims made by previous investigations,[8−12,16,17] we have found that Kraton G1650 did not play the role of an effective compatibilizing agent when melt blended with hPS and PP at 200 °C, which is far below the T_{ODT} (>350 °C) of Kraton G1650. When the PS blocks in Kraton G1650 stay in the form of microdomains at $T < T_{ODT}$, there is little possibility for interdiffusion to take place, during melt blending, between PS-220 and PS blocks of Kraton G1650, because at the melt blending temperature employed (200 °C) the viscosity of Kraton G1650 is exceedingly high (a few orders of magnitude) compared to the viscosity of PS-220. There is ample experimental evidence showing that the viscosity of a block copolymer is very high at $T < T_{ODT}$ and becomes significantly reduced at $T > T_{ODT}$.[46,47] This then suggests that, for effective compatibilization to occur, SEBS block copolymer be designed in such a way that its T_{ODT} is lower than the melt blending temperature. Thus, from a processing point of view it is highly desirable to have the T_{ODT} of a block copolymer below the melt processing temperature when the block copolymer is to be used as a compatibilizing agent.

Above we have pointed out that the T_{ODT} of a block copolymer is an important processing variable in the compatibilization of a pair of immiscible homopolymers, provided that the thermodynamic requirements are met among the components concerned. Figure 10 gives a schematic diagram depicting the thermodynamic requirements for the compatibilization of a pair of immiscible homopolymers A and B with a C-*block*-D copolymer. That is, in Figure 10 we have assumed that

homopolymer A and block C, and homopolymer B and block D, respectively, have a preferential affinity ($\chi_{AC} < 0$ and $\chi_{BD} < 0$), but homopolymer A and block D, and homopolymer B and block C, respectively, do not have an affinity ($\chi_{AB} > 0$, $\chi_{AD} > 0$, $\chi_{BD} > 0$, and $\chi_{CD} > 0$). However, even if homopolymer A and block C, and homopolymer B and block D, respectively, have preferential affinity, the molecular weight of each component plays an important role in the rate of formation of an interphase. Specifically, a block copolymer will act as an effective compatibilizing agent only when the molecular weights of block chains and the corresponding homopolymer lie within a certain range, because the rate of interdiffusion between the components depends on molecular weight. The molecular viscoelasticity theory[48] suggests that the center-of-mass diffusion coefficient (D_0) of a polymer is inversely proportional to molecular weight M (i.e., $D_o \sim 1/M$) for $M < M_c$ and $D_0 \sim 1/M^2$ for $M > M_c$, where M_c is the critical molecular weight for entanglement. This means that when $M > M_c$, the interdiffusion would be very slow. However, from the point of view of mechanical properties, it is highly desirable to have $M > M_c$, so that the chains would not be easily pulled out from the interphase when an external force is applied.

It is well-established today that the T_{ODT} of a block copolymer depends on the molecular weight and the composition of a block copolymer.[40,49] What is urgently in need is a comprehensive theory, which will enable one to predict, during melt processing, the "width of interphase" in an A/B/(C-*block*-D) ternary blend as a function of the molecular weights of homopolymers A and B, the molecular weight and block length ratio of the C-*block*-D copolymer, blend composition, and the interaction parameters, which in turn depend on temperature, for each pair of the components concerned. Note that the A/B/(A-*block*-B), A/B/(A-*block*-D), or A/B/(C-*block*-B) ternary system can be treated as a special case of the A/B/(C-*block*-D) ternary system. When such a theory becomes available, one can avoid otherwise very time-consuming and costly, sometimes unnecessary, experiments.

We wish to point out that A-*block*-B copolymer in A/B/(A-*block*-B) ternary blends may not function as an effective compatibilizing agent even when melt blending is conducted at temperatures above the T_{ODT} of the A-*block*-B copolymer. This observation is illustrated in Figure 11, where TEM micrographs of 63/27/10 (PS-220)/(PI-200)/(SI-9/9) and 63/27/10 (PS-220)/(PB-80)/(SB-9/8) ternary blends, each annealed for 12 h at a temperature above the T_{ODT} of the respective block copolymer (SI-9/9 or SB-9/8), are shown. Note that both 63/27/10 (PS-220)/(PI-200)/(SI-9/9) and 63/27/10 (PS-220)/(PB-80)/(SB-9/8) ternary blends belong to the A/B/(A-*block*-B) ternary system. It can be seen in Figure 11 that the block copolymer, SI-9/9 or SB-9/8, forms a separate phase, maintaining lamellar microdomain structure, inside the droplet of a homopolymer (PI-200 or PB-80). There is little evidence indicating that the block copolymer (SI-9/9 or SB-9/8) is distributed uniformly on the surface of the droplet that is dispersed in the PS-220 matrix. This observation seems to suggest that (i) A-*block*-D copolymer in A/B/(A-*block*-D) ternary blends with $\chi_{BD} < 0$, (ii) C-*block*-B copolymer in A/B/(C-*block*-B) ternary blends with $\chi_{AC} < 0$, and (iii) C-*block*-D copolymer in A/B/(C-*block*-D) ternary blends with $\chi_{AC} < 0$ and $\chi_{BD} < 0$ would be much more effective in the compatibilization of A/B binary blends with $\chi_{AB} > 0$ than A-*block*-B copolymer might be. The above conclusion is consistent with the recent studies of Adedeji et al.,[50,51] who demonstrated that the effective emulsification of two immiscible homopolymers or random copolymers using an AB-type diblock copolymer requires attractive thermodynamic interactions (i.e., negative χ values) between the homopolymer or random copolymer and the corresponding block in the AB-type diblock copolymer.

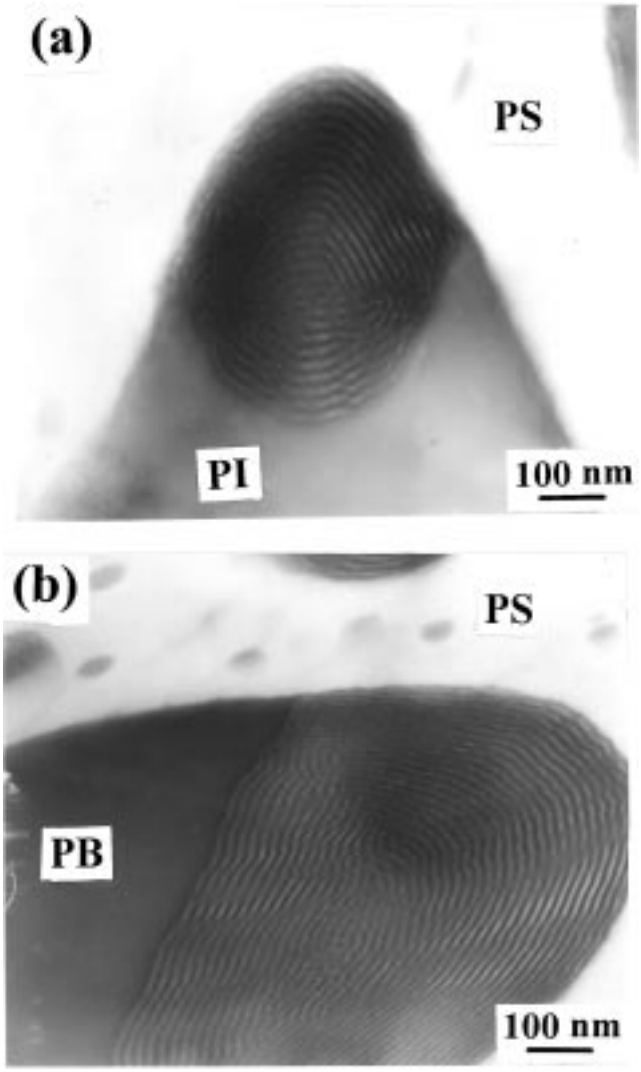

Figure 11. (a) TEM image of the 63/27/10 (PS-220)/(PI-200)/(SI-9/9) ternary blend annealed at 160 °C (above the T_{ODT} of SI-9/9) for 12 h, where the block copolymer SI-9/9 maintains lamellar microdomain structure inside a PI-200 droplet. (b) TEM image of the 63/27/10 (PS-220)/(PB-80)/(SB-9/8) ternary blend annealed at 160 °C (above the T_{ODT} of SB-9/8) for 12 h, where the block copolymer SB-9/8 maintains lamellar microdomain structure inside a PB-80 droplet.

References and Notes

(1) Noolandi, J.; Hong, K. M. *Macromolecules* **1984**, *17*, 1531.
(2) Leibler, L. *Makromol. Chem. Macromol. Symp.* **1988**, *16*, 1.
(3) Noolandi, J. *Makromol. Chem. Rapid Commun.* **1991**, *12*, 517.
(4) Shull, K. R.; Kramer, E. J. *Macromolecules* **1990**, *23*, 4769.
(5) Banaszak, M.; Whitmore, M. D. *Macromolecules* **1992**, *25*, 249.
(6) Banaszak, M.; Whitmore, M. D. *Macromolecules* **1992**, *25*, 2757.
(7) Vilgis, T. A.; Noolandi, J. *Macromolecules* **1990**, *23*, 2941.

(8) Traugott, T. D.; Barlow, J. W.; Paul, D. R. *J. Appl. Polym. Sci.* **1983**, *28*, 2947.
(9) Barlow, J. W.; Paul, D. R. *Polym. Eng. Sci.* **1984**, *24*, 525.
(10) Schwarz, M. C.; Barlow, J. W.; Paul, D. R. *J. Appl. Polym. Sci.* **1988**, *35*, 2053.
(11) Schwarz, M. C.; Barlow, J. W.; Paul, D. R. *J. Appl. Polym. Sci.* **1989**, *37*, 403.
(12) Park, I.; Barlow, J. W.; Paul, D. R. *J. Appl. Polym. Sci.* **1992**, *45*, 1313.
(13) Ouhadi, T.; Fayt, R.; Jérôme, R.; Teyssie, Ph. *J. Polym. Sci., Polym. Phys. Ed.* **1986**, *24*, 973.
(14) Fayt, R.; Jérôme, R.; Teyssie, Ph. *J. Polym. Sci., Polym. Phys. Ed.* **1989**, *27*, 775.
(15) Fayt, R.; Teyssie, Ph. *Polym. Eng. Sci.* **1989**, *29*, 538.
(16) Gupta, A. K.; Purwar, S. N. *J. Appl. Polym. Sci.* **1985**, *30*, 1799.
(17) Srinivasan, K. R.; Gupta, A. K. *J. Appl. Polym. Sci.* **1994**, *53*, 1.
(18) Jo, W. H.; Kim, H. C.; Baek, D. H. *Macromolecules* **1991**, *24*, 2231.
(19) Jo, W. H.; Jo, B. C.; Cho, J. C. *J. Polym. Sci., Polym. Phys. Ed.* **1994**, *32*, 1661.
(20) Auschra, C.; Stadler, R.; Voight-Martin, I. G. *Polymer* **1993**, *34*, 2081, 2094.
(21) Setz, S.; Stricker, F.; Kressler, J.; Duschek, T.; Mülhaupt, R. *J. Appl. Polym. Sci.* **1996**, *59*, 1117.
(22) Heck, B.; Arends, P.; Ganter, M.; Kressler, J.; Stühn, B. *Macromolecules* **1997**, *30*, 4559.
(23) Brown, H. R.; Char, K.; Deline, V. R.; Green, P. F. *Macromolecules* **1993**, *26*, 4155.
(24) Char, K.; Brown, H. R.; Deline, V. R. *Macromolecules* **1993**, *26*, 4164.
(25) Reichert, W. F.; Brown, H. R. *Polymer* **1993**, *34*, 2291.
(26) Creton, C.; Kramer, E. J.; Hui, C. Y.; Brown, H. R. *Macromolecules* **1992**, *25*, 3075.
(27) Edgecombe, B. D.; Stein, J. A.; Frechet, M. J.; Xu, Z.; Kramer, E. J. *Macromolecules* **1998**, *31*, 1292.
(28) Helfand, E.; Tagami, Y. *J. Polym. Sci., Polym. Lett.* **1971**, *9*, 741.
(29) Helfand, E.; Tagami, Y. *J. Chem. Phys.* **1972**, *56*, 359; **1972**, *57*, 1812.
(30) Broseta, D.; Fredrickson, G. H.; Helfand, E.; Leibler, L. *Macromolecules* **1990**, *23*, 132.
(31) Recently, Neumann et al. (ref 32) referred to the log G' vs log G'' plot as the Han plot. It was Han who in 1982 first reported that log G' vs log G'' plots show temperature independence for homopolymers (ref 33). The Han plot has as its basis a molecular viscoelasticity theory for monodisperse homopolymers (ref 34a) and also for polydisperse homopolymers (ref 34b). Since then, the Han plot has very successfully been used to determine the T_{ODT} of microphase-separated block copolymer (refs 35, 36). It should be pointed out that the Han plot has no relation whatsoever to the Cole−Cole plot (ref 37), because the Cole−Cole plot uses the rectangular coordinates showing a semicircle with temperature dependence.
(32) Neumann, C.; Loveday, D. R.; Abetz, V.; Stadler, R. *Macromolecules* **1998**, *31*, 2493.
(33) Han, C. D.; Lem, K. W. *Polym. Eng. Rev.* **1982**, *2*, 135.
(34) (a) Han, C. D.; Jhon, M. S. *J. Appl. Polym. Sci.* **1986**, *32*, 3809. (b) Han, C. D.; Kim, J. K. *Macromolecules* **1989**, *22*, 4292.
(35) (a) Han, C. D.; Kim, J. *J. Polym. Sci., Polym. Phys. Ed.* **1987**, *25*, 1741. (b) Han, C. D.; Kim, J.; Kim, J. K. *Macromolecules* **1989**, *22*, 383. (c) Han, C. D.; Baek, D. M.; Kim, J. K. *Macromolecules* **1990**, *23*, 561.
(36) Han, C. D.; Baek, D. M.; Kim, J. K.; Ogawa, T.; Sakamoto, N.; Hashimoto, T. *Macromolecules* **1995**, *28*, 5043.
(37) Cole, K. S.; Cole, R. H. *J. Chem. Phys.* **1941**, *9*, 341.
(38) Gouinlock, E. V.; Porter, R. S. *Polym. Eng. Sci.* **1977**, *17*, 535.
(39) Chung, C. I.; Lin, M. I. *J. Polym. Sci., Polym. Phys. Ed.* **1978**, *16*, 545.
(40) Helfand, E.; Wasserman, Z. R. In *Developments in Block Copolymers*; Goodman, I., Ed.; Applied Science: New York, 1982; Chapter 4.
(41) Han, C. D.; Chun, S. B.; Hahn, F. S.; Harper, S. Q.; Savickas, P, J.; Meunier, D. J.; Li, L.; Yalcin, T. *Macromolecules* **1998**, *31*, 394.
(42) Yang, K.; Han, C. D. *Polymer* **1996**, *37*, 5795.
(43) Lee, J. K.; Han, C. D. *Polymer* **1999**, *40*, 2521.
(44) Thudium, R. N.; Han, C. C. *Macromolecules* **1996**, *29*, 2143.
(45) Takeno, H.; Hashimoto, *J. Chem. Phys.* **1997**, *107*, 1634.
(46) Ghijsels, A.; Raadsen, J. *Pure Appl. Chem.* **1980**, *52*, 1359.
(47) Han, C. D.; Baek, D. M.; Kim, J. K.; Chu, S. G. *Polymer* **1992**, *33*, 294.
(48) Doi, M.; Edwards, S. F. *The Theory of Polymer Dynamics*; Clarendon Press: Oxford, 1986.
(49) Leibler, L. *Macromolecules* **1980**, *13*, 1602.
(50) Adedeji, A.; Hudson, S. D.; Jamieson, A. M. *Polymer* **1997**, *38*, 737.
(51) Adedeji, A.; Jamieson, A. M.; Hudson, S. D. *Polymer* **1997**, *38*, 2753.

MA981665C